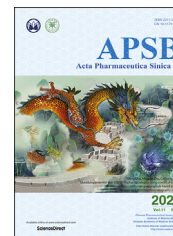




Chinese Pharmaceutical Association  
Institute of Materia Medica, Chinese Academy of Medical Sciences

Acta Pharmaceutica Sinica B

[www.elsevier.com/locate/apsb](http://www.elsevier.com/locate/apsb)  
[www.sciencedirect.com](http://www.sciencedirect.com)



ORIGINAL ARTICLE

# Chrysin serves as a novel inhibitor of DGK $\alpha$ /FAK interaction to suppress the malignancy of esophageal squamous cell carcinoma (ESCC)



Jie Chen<sup>†</sup>, Yan Wang<sup>†</sup>, Di Zhao, Lingyuan Zhang, Weimin Zhang, Jiawen Fan, Jinting Li, Qimin Zhan<sup>\*</sup>

Key Laboratory of Carcinogenesis and Translational Research (Ministry of Education/Beijing), Laboratory of Molecular Oncology, Peking University Cancer Hospital & Institute, Beijing 100142, China

Received 15 March 2020; received in revised form 12 May 2020; accepted 26 June 2020

## KEY WORDS

Chrysin;  
Esophageal squamous cell carcinoma;  
DGK $\alpha$ ;  
FAK;  
Protein–protein interactions

**Abstract** Among current novel druggable targets, protein–protein interactions (PPIs) are of considerable and growing interest. Diacylglycerol kinase  $\alpha$  (DGK $\alpha$ ) interacts with focal adhesion kinase (FAK) band 4.1-ezrin-radixin-moesin (FERM) domain to induce the phosphorylation of FAK Tyr397 site and promotes the malignant progression of esophageal squamous cell carcinoma (ESCC) cells. Chrysin is a multi-functional bioactive flavonoid, and possesses potential anticancer activity, whereas little is known about the anticancer activity and exact molecular mechanisms of chrysin in ESCC treatment. In this study, we found that chrysin significantly disrupted the DGK $\alpha$ /FAK signalosome to inhibit FAK-controlled signaling pathways and the malignant progression of ESCC cells both *in vitro* and *in vivo*, whereas produced no toxicity to the normal cells. Molecular validation specifically demonstrated that Asp435 site in the catalytic domain of DGK $\alpha$  contributed to chrysin-mediated inhibition of the assembly of DGK $\alpha$ /FAK complex. This study has illustrated DGK $\alpha$ /FAK complex as a target of chrysin for the first time, and provided a direction for the development of natural products-derived PPIs inhibitors in tumor treatment.

**Abbreviations:** DGK $\alpha$ , diacylglycerol kinase  $\alpha$ ; ELISA, enzyme-linked immunosorbent assay; ESCC, esophageal squamous cell carcinoma; FAK, focal adhesion kinase; IB, immunoblotting; IP, immunoprecipitation; PPIs, protein–protein interactions.

<sup>\*</sup>Corresponding author.

E-mail address: [zhanqimin@bjmu.edu.cn](mailto:zhanqimin@bjmu.edu.cn) (Qimin Zhan).

<sup>†</sup>These authors made equal contributions to this work.

Peer review under responsibility of Chinese Pharmaceutical Association and Institute of Materia Medica, Chinese Academy of Medical Sciences.

<https://doi.org/10.1016/j.apsb.2020.07.011>

2211-3835 © 2021 Chinese Pharmaceutical Association and Institute of Materia Medica, Chinese Academy of Medical Sciences. Production and hosting by Elsevier B.V. This is an open access article under the CC BY-NC-ND license (<http://creativecommons.org/licenses/by-nc-nd/4.0/>).

## 1. Introduction

Esophageal squamous cell carcinoma (ESCC) is one of the most common malignancies worldwide and occurs at a relatively high frequency in China<sup>1</sup>. Although recent advances in chemotherapy with platinum agents or other cytotoxic agents have yielded modest improvements in ESCC patient outcomes, the 5-year overall survival rate remains poor due to the limited understanding on the complicated molecular mechanism in ESCC cells and lack of more efficient therapeutic approaches<sup>2</sup>. Therefore, novel effective and promising treatment targets and strategies need to be explored urgently.

Focal adhesion kinase (FAK), a cytoplasmic nonreceptor tyrosine kinase encoded by *PTK2*, is dysregulated in several tumors and correlated with poor clinical outcome, especially in ESCC<sup>3–5</sup>. FAK promotes the proliferation, survival, invasion and stemness of ESCC cells. Inhibition of FAK activity produces beneficial effect on ESCC cells. Protein–protein interactions (PPIs) are essential for high-affinity binding between proteins, and contribute to explore specific inhibitors in tumor treatment. Several inhibitors of FAK-based PPIs have been developed. A peptide targeting 7-amino acid residues in the N-terminal proline-rich domain (located in FERM domain) of FAK blocked the interaction between FAK and P53, and showed excellent antitumor activity in breast and colon cancers<sup>6</sup>. Another study identified that 5'-*O*-tritylthymidine (M13 compound) docked into the pocket of FAK FERM domain and inhibited FAK/mouse double minute-2 (MDM-2) interaction and tumor malignancy of several cancers<sup>7</sup>. Our previous study had found that diacylglycerol kinase  $\alpha$  (DGK $\alpha$ ), an oncogenic protein, interacts with FAK FERM domain to assemble the DGK $\alpha$ /FAK complex and induce the phosphorylation of FAK Tyr397 site in ESCC cells<sup>5</sup>. Thus, demonstrating whether the DGK $\alpha$ /FAK complex can be used as the druggable PPI is critically for the development of therapeutic agents in ESCC treatment.

Natural products, especially flavonoids, possessing diverse bioactivities and mechanisms usually serve as excellent lead compounds for cancer prevention and anticancer drug discovery<sup>8–10</sup>. We screened 63 natural flavonoids and identified that chrysin, a natural flavonoid from *Passiflora caerulea*, shows excellent inhibitory effect on the malignant progression of ESCC cells. Accumulating evidences have suggested that chrysin harbors anticancer activities, including inhibition of tumor growth, induction of apoptosis, and reduction of inflammation, with low adverse effects and toxicity, making it safe for clinical use<sup>11–13</sup>. Here, we investigated the effect of chrysin on several malignant phenotypes of ESCC cells and explored the underlying mechanisms.

## 2. Materials and methods

### 2.1. Reagents and antibodies

Antibody against DGK $\alpha$  (Cat# H00001606–B01P) was from Abnova (Taipei, Taiwan, China). Antibody against FAK (N-terminal, Cat# sc-557) was from Santa Cruz Biotechnology (Santa Cruz, CA, USA). Antibodies against pFAK Tyr397 (Cat# 3283S), Janus kinase 2 (JAK2, Cat# 3230), phosphoJAK2 (pJAK2) Tyr1007/1008 (Cat# 3771), Janus kinase 3 (JAK3, Cat# 8827),

pJAK3 Tyr980/981 (Cat# 5031), glyceraldehyde-3-phosphate dehydrogenase (GAPDH, Cat# 5174), protein kinase B (AKT, Cat# 4691), pAKT Ser473 (Cat# 4060), and pFAK Tyr397 (Cat# 3283S) were from Cell Signaling Technology (Danvers, MA, USA). Z-Val-Ala-Asp-FMK (Z-VAD-FMK, Cat# S7023), and PF562271 (Cat# S2890) were from Selleck Chemicals (Houston, TX, USA). All flavonoids used in the present study were from MedChemExpress (MCE) Inc. (Shanghai, China).

### 2.2. Cell lines and transfection

The human ESCC cell lines, KYSE150, KYSE30, KYSE410, KYSE450, YSE2 and esophageal epithelial cell-SHEE, were originally maintained in Roswell Park Memorial Institute (RPMI) 1640 medium supplemented with 10% fetal bovine serum (FBS), penicillin (100 U/mL), and streptomycin (100  $\mu$ g/mL).

For establishing stable DGK $\alpha$  knockdown ESCC cell lines, KYSE30, KYSE410, and KYSE150 cells were transfected with the pLKO.1 (Addgene, Watertown, MA, USA) and pLKO.1 vector expressing small hairpin (sh) RNA for DGK $\alpha$  knockdown (pLKO.1-shDGK $\alpha$ ). Transfected cells were selected by 0.5  $\mu$ g/mL puromycin. The DGK $\alpha$  shRNA sequences used in present study was according to our previous study<sup>5</sup>. ESCC cells stably expressing Flag-DGK $\alpha$  D435E mutant were generated by transfection of pcDNA3.1/Flag-DGK $\alpha$  D435E plasmid into the indicated ESCC cells and then cultured for 10–14 days with 400  $\mu$ g/mL G418. Point mutation on DGK $\alpha$  was obtained using Phusion<sup>TM</sup> high-fidelity DNA polymerase (Thermo Fisher; Cat# F530L, Waltham, MA, USA). Mutating oligonucleotides were: DGK $\alpha$  D435E CTAGAATCCAGCCTACTGTGCCTTCTCCACC ACACACCAAAATCCG and CGGATTTTGGTGTGTGGTGGGA GAAGGCACAGTAGGCTGGATTCTAG.

### 2.3. Cell proliferation/viability assay

Proliferation/viability of the indicated ESCC cells was determined using 3-(4,5-dimethylthiazol-2-yl)-5-(3-carboxymethoxyphenyl)-2-(4-sulfophenyl)-2H-tetrazolium, inner salt (MTS) method. Briefly,  $5 \times 10^3$  cells in 100  $\mu$ L of RPMI1640 medium were seeded in 96-well plates. Once 90% confluent, cells were treated with the indicated agents for 72 h. Then, the medium was aspirated, and cells were incubated with MTS solution (Promega; Cat# G3582, Madison, WI, USA) for 1 h. The viable cell number was directly proportional to the formazan product, which could be measured spectrophotometrically at 490 nm. For determining half-maximal inhibitory concentration (IC<sub>50</sub>) value of 63 flavonoid natural products in KYSE410 cells, the cell viability measured by MTS in the presence of a wide range of concentrations of these products (0–100  $\mu$ mol/L). For assays determining IC<sub>50</sub> value of chrysin in various ESCC cell lines and SHEE cells, the cell viability measured by MTS in the presence of concentrations from 0 to 50  $\mu$ mol/L.

### 2.4. Colony formation assay

$1 \times 10^3$  cells were seeded into 60 mm dishes in RPMI1640 medium and cultured in the absence or presence of different doses of

chrysin as indicated. After 2 weeks, the cells were washed with phosphate-buffered saline solution (PBS), fixed with methanol and 2% crystal violet. The colonies were counted and then photographed.

### 2.5. Soft agar colony formation assay

$2 \times 10^3$  cells mixed with 1.2% agar solution, 20%  $2 \times$  Dulbecco's modified Eagle's medium (DMEM) solution, and cell suspension were incubated to a 96-well microplate already containing a solidified base agar layer (Cell Biolabs Inc.; Cat# CBA-130, San Diego, CA, USA). After 8-day incubation, lysis buffer was added and the plate was incubated at room temperature for 15 min. Colony formation was quantified using the fluorescent CyQuant staining solution and read in a 96-well fluorometer (Synergy H1, BioTek, Winooski, VT, USA). The experiment was repeated five times.

### 2.6. Invasion assay

The indicated ESCC cells ( $1 \times 10^5$  cells) were placed in the upper chamber of 24-well boyden chambers system (8  $\mu$ m insert) with or without indicated doses of chrysin for 16 h. Then, the cells that invaded to the chamber were fixed and stained with 2% crystal violet solution for 10 min. The invaded cells were then photographed under a microscope (Leica DM2500, Leica, Wetzlar, Germany). The experiment was repeated five times.

### 2.7. Measurements of glucose and lactate

Supernatants from the indicated cells were collected and the glucose and lactate levels were examined using glucose colorimetric assay kit (Biovision, Cat# K686, Palo Alto, CA, USA) and lactate colorimetric assay kit (Biovision, Cat# K627) following the manufacturer's protocols. The experiment was repeated five times.

### 2.8. Flow cytometry (FCM) analysis of apoptosis and caspase activity assay

For evaluating the chrysin-induced apoptosis of ESCC cells, the indicated ESCC cells were incubated in 6-well plates. Then, ESCC cells were treated with different doses of chrysin (10, 25, and 50  $\mu$ mol/L) as indicated for 48 h at 37 °C. The treated ESCC cells were collected and resuspended in the binding buffer provided with the Annexin V-FITC apoptosis detection kit (BD Pharmingen, Cat# 556,547, San Jose, CA, USA). Cells were mixed with 2  $\mu$ L of Annexin V-fluorescein isothiocyanate (FITC) and 5  $\mu$ L of propidium iodide (PI) and incubated for 30 min at 4 °C in the dark. The staining was then terminated and cells were immediately analyzed by flow cytometry (Accuri C6, BD Pharmingen, USA). Caspase 3/7 activity was determined using Caspase-Glo® 3/7 activity system (Progenia; Cat# G8090) according to the manufacturer's instructions. After collecting the indicated ESCC cells, the cell lysates (approximately 50  $\mu$ g) in 50  $\mu$ L volume were mixed with 50  $\mu$ L caspase-Glo 3/7 reagent in 96-well plates and incubated for 1 h at 37 °C in the dark. The luminescence was measured using a plate-reading fluorometer (Synergy H1, BioTek). The experiment was repeated five times.

### 2.9. Antibody arrays

For evaluating chrysin-mediated antesignaling activity in the indicated ESCC cells, lysates were added to Human AKT pathway phosphorylation antibody assay against the phosphorylation status of AKT and RAF proto-oncogene serine/threonine-protein kinase (RAF)/mitogen-activated protein kinase 1 (ERK) pathway proteins (Raybiotech; Cat# AAH-AKT-1-2, Norcross, GA, USA), or human receptor tyrosine kinase (RTK) phosphorylation antibody assay against 71 unique RTKs (Raybiotech; Cat#AAH-PRTK-1-2), and processed according to the manufacturer's instructions. Briefly, membranes were blocked, incubated with approximately 500  $\mu$ L of lysates overnight, followed by biotin-conjugated antibodies (1:250) incubation for 2 h and with horseradish peroxidase (HRP)-linked secondary antibody (1:1000) for 1 h. Then, the membranes were incubated with chemiluminescent substrate and the activation status of signaling proteins was evaluated.

### 2.10. Enzyme-linked immunosorbent assay (ELISA) analysis

The activation of FAK, AKT, ribosomal protein S6 (RPS6), proline-rich AKT1 substrate (PRAS40), or RAF1 both *in vitro* and *in vivo* was respectively analyzed using human pFAK Tyr397 and total FAK ELISA kit (Raybiotech, Cat# PEL-FAK-Y397-T-1), human pAKT Ser473 and total AKT ELISA kit (Raybiotech, Cat# PEL-AKT-S473-T-1), human pRPS6 Ser235/S236 and total RPS6 ELISA kit (Raybiotech, Cat# PEL-RPS6-S235-T-1), human pPRAS40 Thr246 and total PRAS40 ELISA kit (Raybiotech, Cat# PEL-PRAS40-T246-T-1), or human pRAF1 Ser301 and total RAF1 ELISA kit (Raybiotech, Cat# PEL-RAF1-S301-T-1), following the manufacturer's protocols. Briefly, sample lysates were added into appropriated wells of ELISA kits, and incubated for 2 h at 37 °C. Then, discarded these lysates and added 100  $\mu$ L detection antibody solutions to evaluate the expression of phosphorylated or total protein. The activation status of these indicated signaling proteins was evaluated according to the formula that the optical density (OD) value of phosphorylated proteins/the OD value of total proteins.

For measurement of the expression of intracellular biomarkers in the ESCC cells with the indicated treatments, levels of MYC proto-oncogene protein (C-MYC), G1/S-specific cyclin-D1 (cyclin D1), baculoviral IAP repeat-containing protein 5 (survivin), SRY-box transcription factor 2 (SOX2), nanog homeobox (NANOG), POU class 5 homeobox (OCT4), BMI1 proto-oncogene (BMI1), pyruvate kinase M2 (PKM2), hexokinase 2 (HKII), glucose transporter 1 (GLUT1) or lactate dehydrogenase A (LDHA) in the cell lysates were detected using the human C-MYC ELISA kit (Raybiotech; Cat# ELH-CMYC-1), cyclin D1 ELISA kit (Raybiotech; Cat# ELH-CYCD-1), human survivin ELISA kit (Cell Signaling Technology; Cat# 7169C), human SOX2 ELISA kit (Cell Signaling Technology; Cat# 7277C), human NANOG ELISA kit (Raybiotech; Cat# ELH-NANOG-1), human OCT4 ELISA kit (Raybiotech; Cat# ELH-OCT4-1), human BMI1 ELISA kit (Cell Signaling Technology; Cat# 18157C), human PKM2 ELISA kit (Cloud-Clone; Cat# SEA588HU, Wuhan, China), human HKII ELISA kit (Cloud-Clone; Cat# SED352HU), human GLUT1 ELISA kit (Cloud-Clone; Cat# SEB185HU), or human LDHA ELISA kit (Cloud-Clone; Cat# SEB370HU) according to the manufacturer's

instructions. Levels of MMP9 in the supernatants were measured using the human matrix metalloproteinase 9 (MMP9) ELISA Kit (Raybiotech; Cat# ELH-MMP9-1), according to the manufacturer's protocols. The intracellular cleaved poly (ADP-ribose) polymerase (PARP) and caspase 3 in the indicated ESCC cells or tumors were evaluated using the human cleaved PARP (D214/G215) (Raybiotech; Cat# PTE-PARP-D214-1) and cleaved caspase 3 (D175) (Raybiotech; Cat# PTE-CASP3-D175-1) ELISA kits, according to the manufacturer's instructions. The experiment was repeated five times.

## 2.11. Confocal assay

Cells were washed with PBS, fixed in 4% paraformaldehyde, blocked with 5% normal goat serum and incubated with DGK $\alpha$  or FAK antibody (1:200) overnight at 4 °C. Then, cells were stained with tetramethyl rhodamine isothiocyanate (TRITC)- and FITC-conjugated secondary antibody for 1 h at 37 °C. Nuclei were stained with 4',6-diamidino-2-phenylindole (DAPI) at final concentration of 0.1  $\mu$ g/mL. Images were captured and visualized by a confocal microscope (Leica ST2, Leica, Germany).

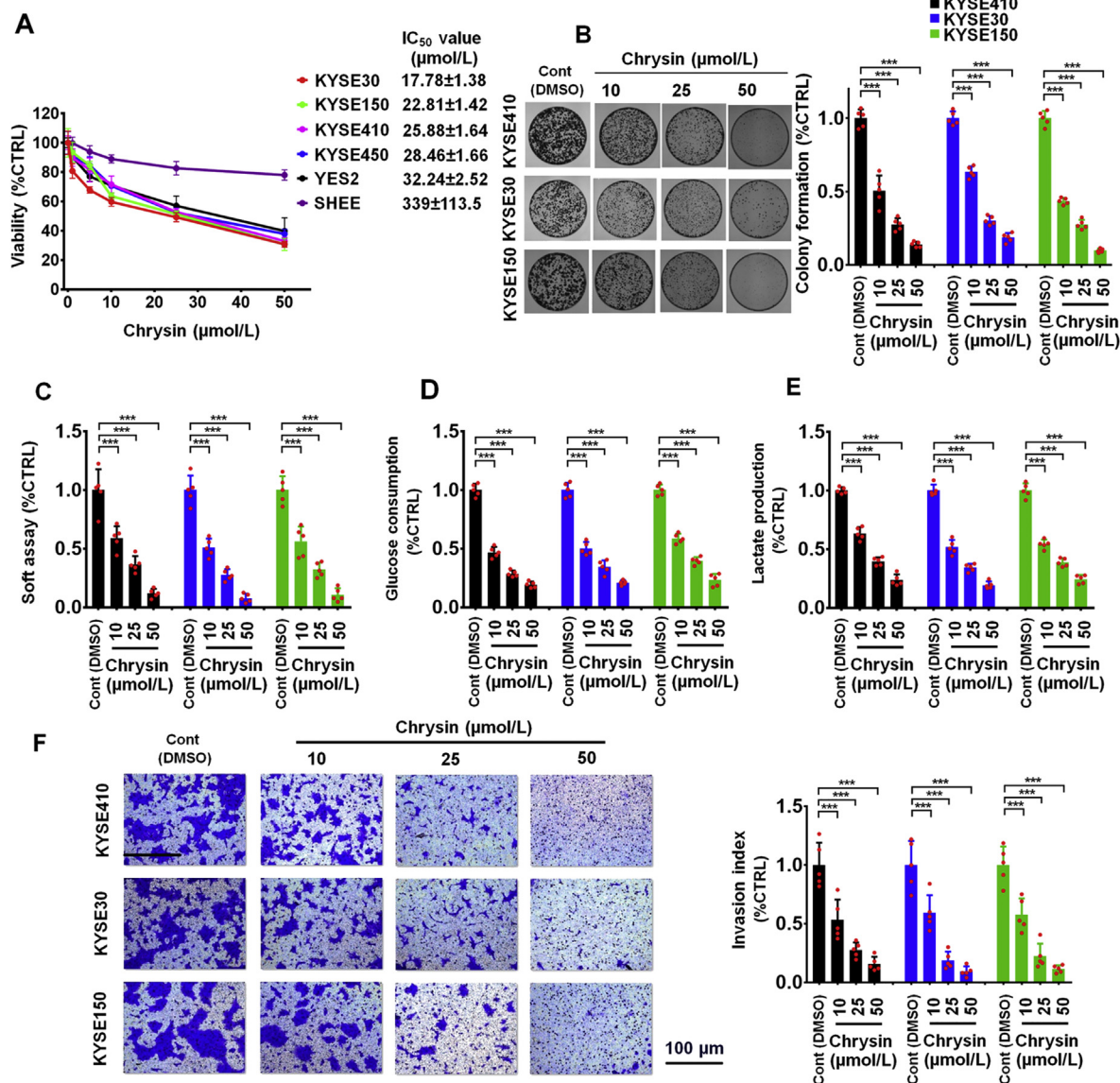


**Figure 1** Chrysin suppresses the malignancy of ESCC cells *in vitro*. (A) The tumor growth inhibitory effect of chrysin on the viability of the indicated ESCC cell lines, including KYSE410, KYSE30, KYSE150, YSE2, KYSE450 and normal esophageal epithelial cells SHEE, was evaluated using MTS assay at the indicated concentration. The IC<sub>50</sub> (mean  $\pm$  SD) of chrysin against these indicated cell lines. (B) Colony formation assay of the indicated ESCC cell lines. Cells were treated with chrysin (10, 25, and 50  $\mu$ mol/L) for 2 weeks. Cells were stained with 2% crystal violet. (C) Effect of chrysin on anchorage-independent growth of the indicated ESCC cells. Cells were treated with the indicated doses of chrysin and incubated for 8 days. Colony formation was quantified using the fluorescent cell stain CyQuant GR Dye. Alteration of glucose consumption (D) and lactate production (E) in control and the indicated doses of chrysin-treated ESCC cells. (F) Alteration of invasive ability in control and the indicated doses of chrysin-treated ESCC cells. Scale bar, 100  $\mu$ m as indicated. Dimethyl sulfoxide (DMSO) was used as the control solvent. \*\*\* $P < 0.001$ . Error bars, mean  $\pm$  SD of three to five independent experiments.

### 2.12. Immunoprecipitation (IP) and immunoblotting (IB) analysis

The indicated cells were washed twice with PBS, lysed in lysis buffer, briefly sonicated, and then subjected to IP-IB assays. For immunoprecipitation, lysates were incubated with the indicated primary antibodies (5  $\mu\text{g}$  antibody/sample) and protein A/G sepharose beads (Thermo; Cat# 20,421) on a rotator (100 rpm) at 4  $^{\circ}\text{C}$  overnight. Then, proteins were separated by sodium dodecyl sulfate (SDS) electrophoresis on the polyacrylamide gel followed by immunoblotting. After overnight incubation with the indicated primary antibodies (diluted at 1:1000; except GAPDH, diluted at 1:3000), at 4  $^{\circ}\text{C}$ , washing and incubation with secondary antibodies, blots were developed with enhanced chemiluminescence assay (Thermo Fisher; Cat# 32,106).

### 2.13. Molecular docking

The DGK $\alpha$  sequence was obtained from UniProt (ID: P23743, <https://www.uniprot.org/uniprot/P23743>). A homology model was produced for DGK $\alpha$  by alignment with the crystal structure of DGK $\alpha$  catalytic domain protein (PDB: 4wer, <https://www.rcsb.org/structure/4wer>) followed by three-dimensional model building and energy minimization using MOE (Molecular Operating Environment, 2015.10, Chemical Computing Group Inc., Canada). The best protein model, including verifying proper assignment of bonds, adding hydrogens, deleting unwanted bound water molecules and minimizing protein energy, was selected for the following studies. Then, ligand (chrysin, PubChem CID: 5281607, <https://pubchem.ncbi.nlm.nih.gov/compound/5281607>) was docked with DGK $\alpha$  catalytic domain using the DOCK, structure preparation, and protonate 3D modules from MOE. The top one

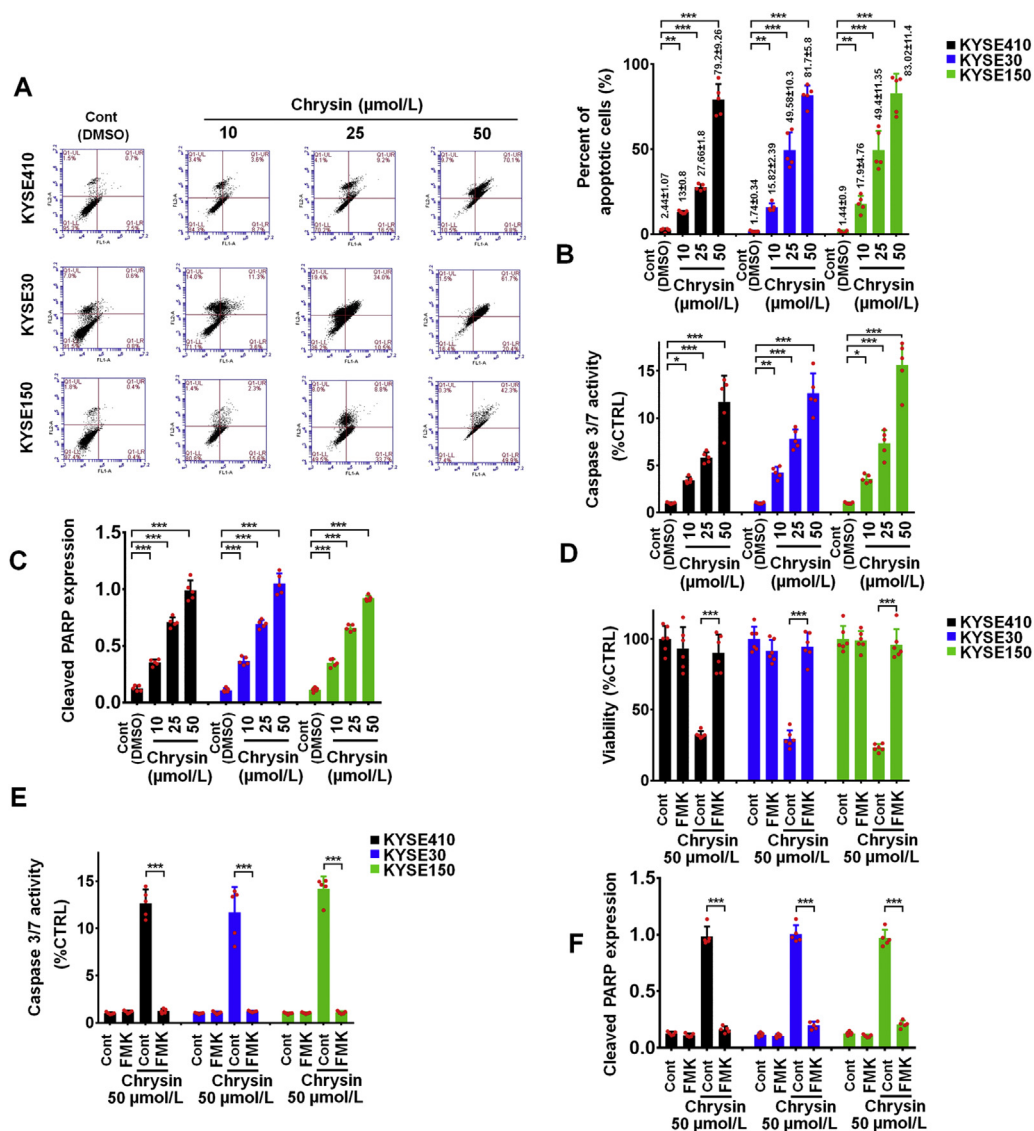


**Figure 2** Chrysin induces the apoptosis of ESCC cells *in vitro*. (A)–(C) The indicated ESCC cells were treated with chrysin (10, 25, and 50  $\mu\text{mol/L}$ ) for 48 h, cell apoptosis was evaluated by FCM assay (values of mean  $\pm$  SD as indicated) (A), caspase 3/7 activity (B), and the cleavage of PARP (C). (D)–(F) The indicated ESCC cells were treated with 50  $\mu\text{mol/L}$  chrysin with and without 50  $\mu\text{mol/L}$  Z-VAD-FMK pretreatment, respectively. Cell viability was measured by MTS assay (D). Apoptosis was evaluated by caspase 3/7 activity (E). The cleavage of PARP was measured by ELISA assay (F). \* $P < 0.05$ , \*\* $P < 0.01$ , \*\*\* $P < 0.001$ . Error bars, mean  $\pm$  SD of five independent experiments.

ranking affinity pose was chosen as the final pose of chrysin/DGK $\alpha$  catalytic domain interaction.

### 2.14. Xenograft studies

The animal experiment was approved by the animal handling and procedures were approved by the Animal Center, Peking University Cancer Hospital & Institute (Beijing, China). KYSE410, KYSE30 and KYSE150 cells (approximately  $2.5 \times 10^6$  cells) in 100  $\mu$ L PBS were subcutaneously inoculated into the right flank of 5-week-old female BALB/c nude mice (Vital River Laboratories, Beijing, China). Treatment was initiated when tumors reached 80–100 mm<sup>3</sup>. The drug efficacy study was performed with four groups according to different doses of chrysin, including control, chrysin (10, 25, or 50 mg/kg/day, *p.o.*;  $n = 5$ /group). The selected dosage and administration are referred to previous reports<sup>13–16</sup>. Animals were randomized to receive control solvent and different doses of chrysin. Eq. (1) was used to evaluate the tumor size:

$$\text{Tumor size (mm}^3\text{)} = (\text{Length} \times \text{Width}^2) \times 0.5 \quad (1)$$

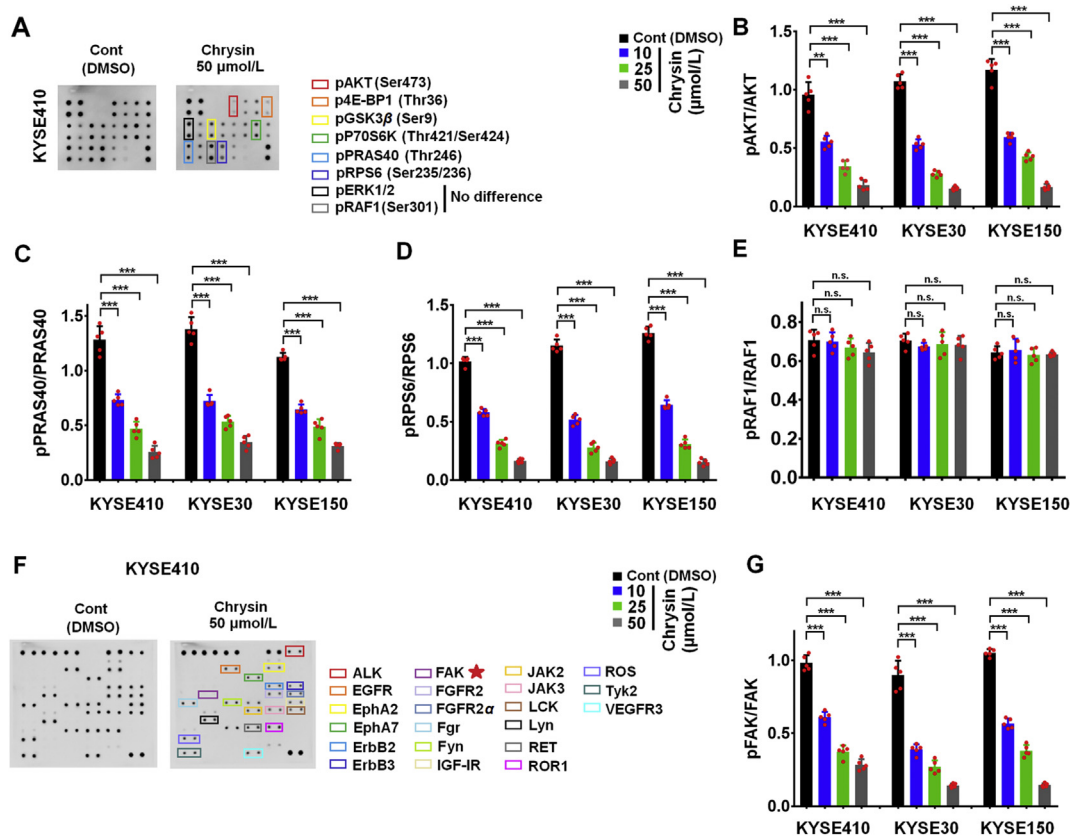


**Figure 3** Chrysin inhibits ESCC malignancy *via* suppressing the activation of FAK/AKT signaling. The indicated ESCC cells were treated with 50  $\mu$ mol/L chrysin, and then the activation of AKT or RAF/ERK signaling were analyzed using antibody array. No difference of pRAF1 Ser<sup>301</sup> expression was indicated between control group and 50  $\mu$ mol/L chrysin group. (B)–(E) The indicated ESCC cells were treated with chrysin (10, 25, and 50  $\mu$ mol/L) for 4 h, the activation of pAKT Ser<sup>473</sup> (B), pPRAS40 Thr<sup>246</sup> (C), pRPS6 Ser<sup>235/236</sup> (D) and pRAF1 Ser<sup>301</sup> (E) was evaluated by quantitative ELISA assay. (F) Total protein lysates from the indicated cells treated with 50  $\mu$ mol/L chrysin were analyzed using antibody array against 71 tyrosine kinases. (G) The indicated ESCC cells were treated with chrysin (10, 25, and 50  $\mu$ mol/L) for 4 h, the activation of pFAK Tyr<sup>397</sup> was evaluated by quantitative ELISA assay. n.s., no significant difference, \*\* $P < 0.01$ , \*\*\* $P < 0.001$ . Error bars, mean  $\pm$  SD of five independent experiments.

### 2.15. Statistical analysis

All experiments but not statistical analysis are randomized and blinded. For all assays in the present study, three to five independent repeat experiments were carried out. All statistical analyses were conducted using GraphPad Prism version 7.0 (GraphPad Software Inc., La Jolla, CA, USA). Experimental data were analyzed by one-way analysis of variance (ANOVA) followed by Dunnett's *post hoc* test when comparing more than two groups of data and one-way ANOVA, non-parametric Kruskal–Wallis test followed by Dunnett's *post hoc* test was used when comparing multiple independent groups. All data are presented as the mean  $\pm$  standard deviation (SD). A  $P$  value of less than 0.05 was considered significant.

## 3. Results

### 3.1. Chrysin inhibits malignant progression of ESCC cells

Supporting Information Table S1 indicates the IC<sub>50</sub> values of 63 flavonoid natural products in ESCC cell line-KYSE410 using MTS assay. Chrysin was chosen for further studies due to its excellent antitumor effect and low toxicity<sup>11–13</sup>. Fig. 1A shows that chrysin

treatment for 72 h significantly reduced the viability of five different ESCC cell lines in a dose-dependent manner determined by MTS assay with the indicated  $IC_{50}$  value ranging from 17.78 to 32.24  $\mu\text{mol/L}$ . However, chrysin had little cytotoxicity in esophageal epithelial cell-SHEE with the same concentration ranges used in ESCC cell lines. Anchorage-dependent colony formation assay was used to evaluate the long-term growth inhibitory effect of chrysin on ESCC cells. As shown in Fig. 1B, chrysin dose-dependently suppressed the anchorage-dependent colony formation of ESCC cells. We further evaluated the effect of chrysin on other malignant phenotypes, such as stemness, glycolysis, or

invasive ability in ESCC cells. Soft agar assay was applied to examine the effect of chrysin on anchorage-independent growth ability of ESCC cells. Fig. 1C shows that chrysin dose-dependently inhibited the soft agar-based colony formation in the ESCC cells, after 8 days incubation. Glycolysis provides energy for tumor malignant progression, we next investigated whether chrysin downregulated ESCC glycolysis. Chrysin significantly reduced the levels of glycolytic indexes, such as glucose uptake (Fig. 1D) and lactate production (Fig. 1E) compared with control ESCC cells. Fig. 1F shows that chrysin dose-dependently inhibited the invasion of the indicated ESCC cells.

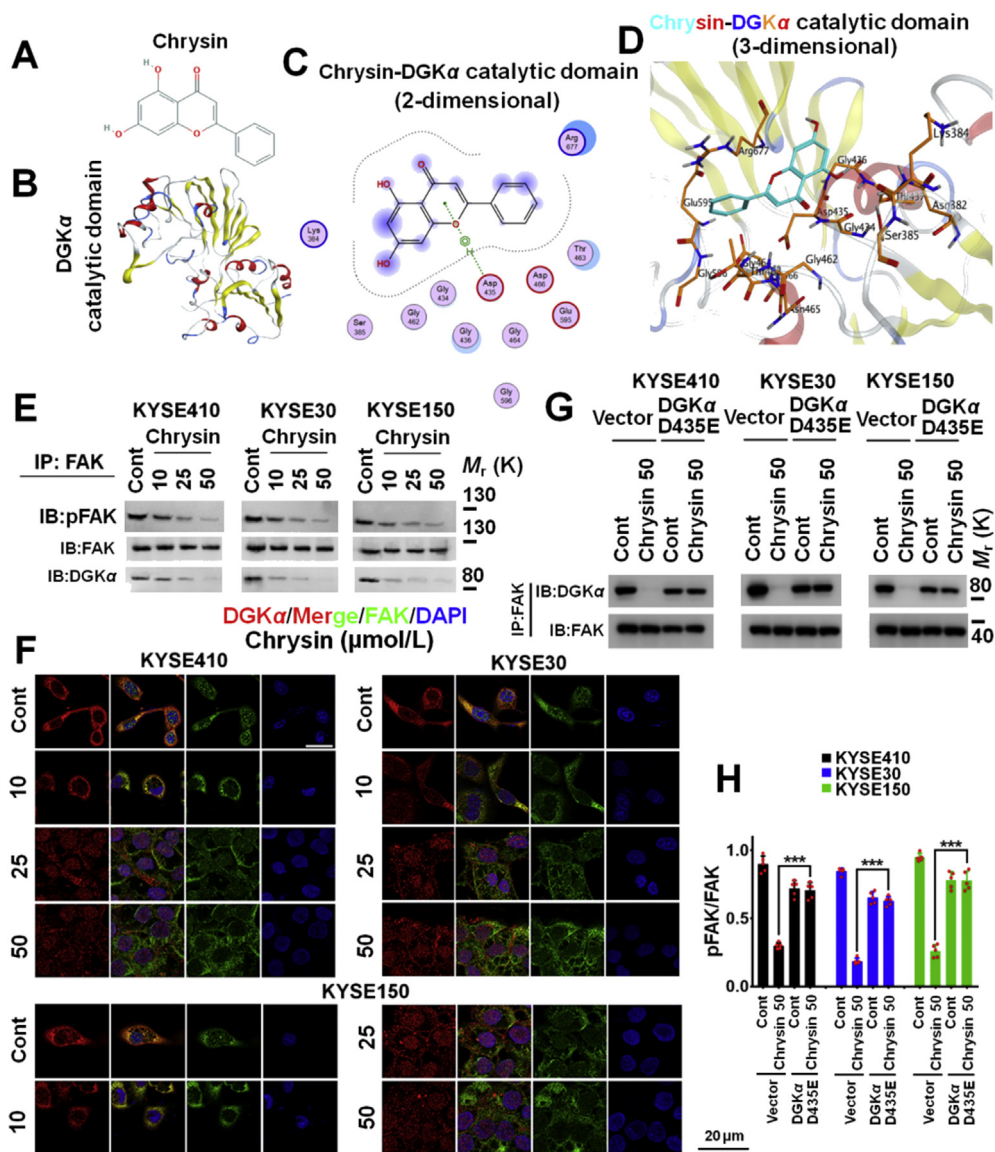


**Figure 4** Chrysin interacts with DGK $\alpha$  to inhibit the activation of FAK/AKT signaling. The structure of chrysin (A) and 3-dimensional structure of DGK $\alpha$  catalytic domain (B). 2- (C) or 3-Dimensional (D) structure of docking of chrysin to the Asp<sup>435</sup> site in the catalytic domain of DGK $\alpha$ . (E) The indicated ESCC cells were treated with chrysin (10, 25, and 50  $\mu\text{mol/L}$ ) for 2 h. The interaction between DGK $\alpha$  and FAK, or the activation of FAK in DGK $\alpha$ /FAK complex was assayed using IP (IP: FAK) and IB (IB: FAK, pFAK, or DGK $\alpha$ ) analysis (E). (F) The indicated ESCC cells were treated with chrysin (10, 25, and 50  $\mu\text{mol/L}$ ) for 2 h. The interaction between DGK $\alpha$  and FAK was evaluated using confocal assay. Cells were stained with DAPI to visualize the nucleus. Scale bar, 20  $\mu\text{m}$  as indicated. (G) and (H) The indicated ESCC cells were treated with 50  $\mu\text{mol/L}$  chrysin. The interaction between DGK $\alpha$  and FAK was evaluated using IP (IP: FAK) and IB (IB: FAK, or DGK $\alpha$ ) assay after 2-h treatment (G), and the phosphorylation of FAK Tyr<sup>397</sup> was evaluated using quantitative ELISA assay after 4-h treatment (H). \*\*\* $P < 0.001$ . Error bars, mean  $\pm$  SD of five independent experiments.

### 3.2. Chrysin promotes the apoptosis of ESCC cells via caspase-dependent pathway

We investigated the apoptosis-promoting effect of chrysin on ESCC cells. As shown in Fig. 2A and B, chrysin dose-dependently increased the apoptotic rate and caspase 3/7 activity in KYSE410, KYSE30, and KYSE150 cells. Consistently, a similar trend was reflected in the cleavage of apoptotic biomarker-PARP (Fig. 2C).

To assess the significance of caspases activation in chrysin-induced apoptosis, ESCC cells were pretreated with 50  $\mu\text{mol/L}$  Z-VAD-FMK, a pan-caspase inhibitor, which was employed to block caspase activation. Fig. 2D shows that Z-VAD-FMK greatly attenuated the effect of chrysin-mediated growth inhibition. Z-VAD-FMK incubation also abolished the stimulatory effect of chrysin on the caspase 3/7 activity (Fig. 2E) and the cleaved PARP expression (Fig. 2F). Taken together, these results suggest that chrysin-induced apoptosis is majorly dependent on caspase activation in ESCC cells.

### 3.3. Chrysin inhibits the FAK/AKT pathway in ESCC cells

The antibody array was used to evaluate the inhibitory effect of chrysin on AKT and ERK signaling pathways, which greatly

contribute to the malignant progression of ESCC cells<sup>5,17,18</sup>. Fig. 3A shows that 50  $\mu\text{mol/L}$  chrysin effectively inhibited the activation of pAKT Ser<sup>473</sup> and its downstream substrates, including pRPS6 Ser<sup>235/236</sup> and pPRAS40 Thr<sup>246</sup> in KYSE410 cells. However, 50  $\mu\text{mol/L}$  chrysin produced minimal inhibitory effect on the activation of pRAF1 Ser<sup>301</sup> in KYSE410 cells (Fig. 3A). Quantitative ELISA assays confirm the above results and further show that chrysin dose-dependently inhibited the phosphorylation of AKT (Fig. 3B and Supporting Information Fig. S1), PRAS40 (Fig. 3C) or RPS6 (Fig. 3D), whereas not RAF1 (Fig. 3E) in the indicated ESCC cells.

Then, the “phospho-activated” protein tyrosine kinases (PTKs) antibody array was used to evaluate the inhibitory effect of chrysin on the activation of upstream protein kinases. Fig. 3F shows that 50  $\mu\text{mol/L}$  chrysin most effectively inhibited the phosphorylation of FAK Tyr397 among these PTKs. Quantitative ELISA assay confirms the above results and also finds that chrysin dose-dependently suppressed the phosphorylation of FAK Tyr397 in the indicated ESCC cells (Fig. 3G and Supporting Information Fig. S2). JAK2 and JAK3 are the two important targeted proteins that contribute to tumor malignancy, including ESCC<sup>19,20,21</sup>. Fig. 3F shows that 50  $\mu\text{mol/L}$  chrysin could also suppress the phosphorylation of JAK2 and JAK3. Supporting Information

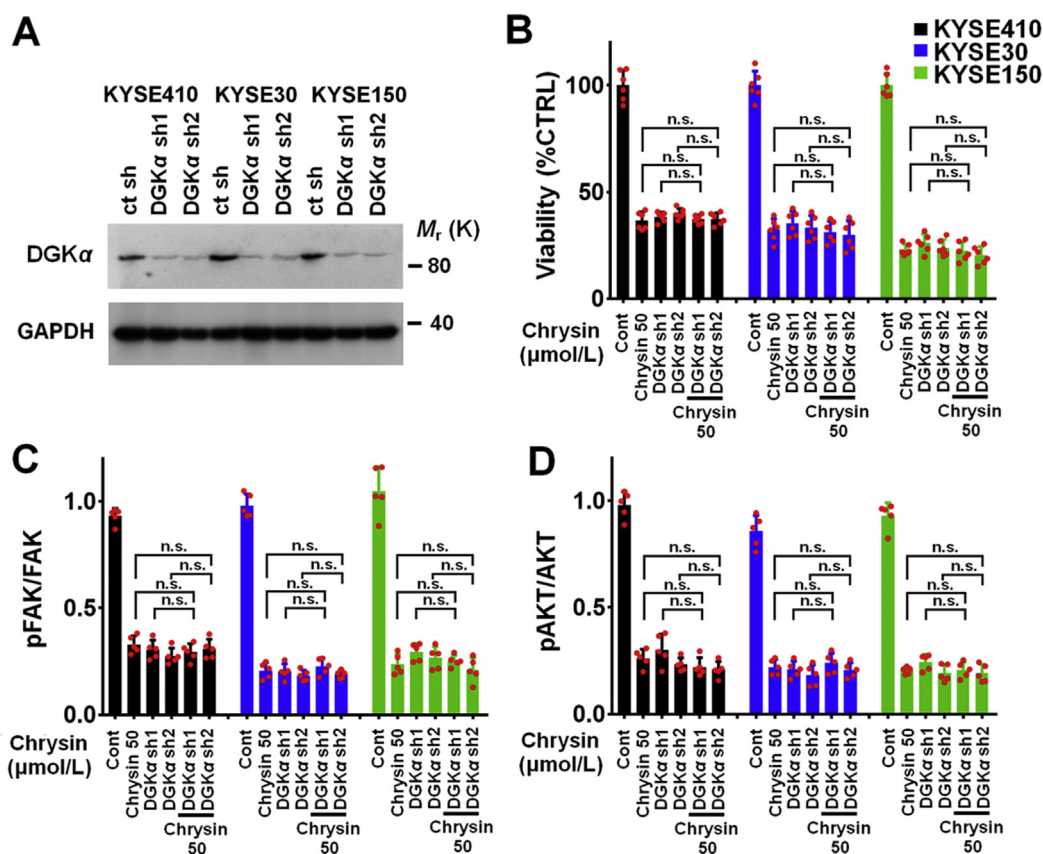


**Figure 5** DGK $\alpha$  is critical for chrysin-mediated tumor inhibitory effect and FAK/AKT signaling inhibition. Stable silencing DGK $\alpha$  in 2 specific shRNA-transduced ESCC cell lines analyzed by immunoblotting. GAPDH was used as a loading control. (B)–(D) The indicated control or DGK $\alpha$  shRNA ESCC cells were treated with 50  $\mu\text{mol/L}$  chrysin. Then, the growth ability of ESCC cells was observed by MTS assay (B). The activation of FAK (C) and AKT (D) was evaluated using quantitative ELISA assay. n.s., no significant difference. Error bars, mean  $\pm$  SD of five independent experiments.

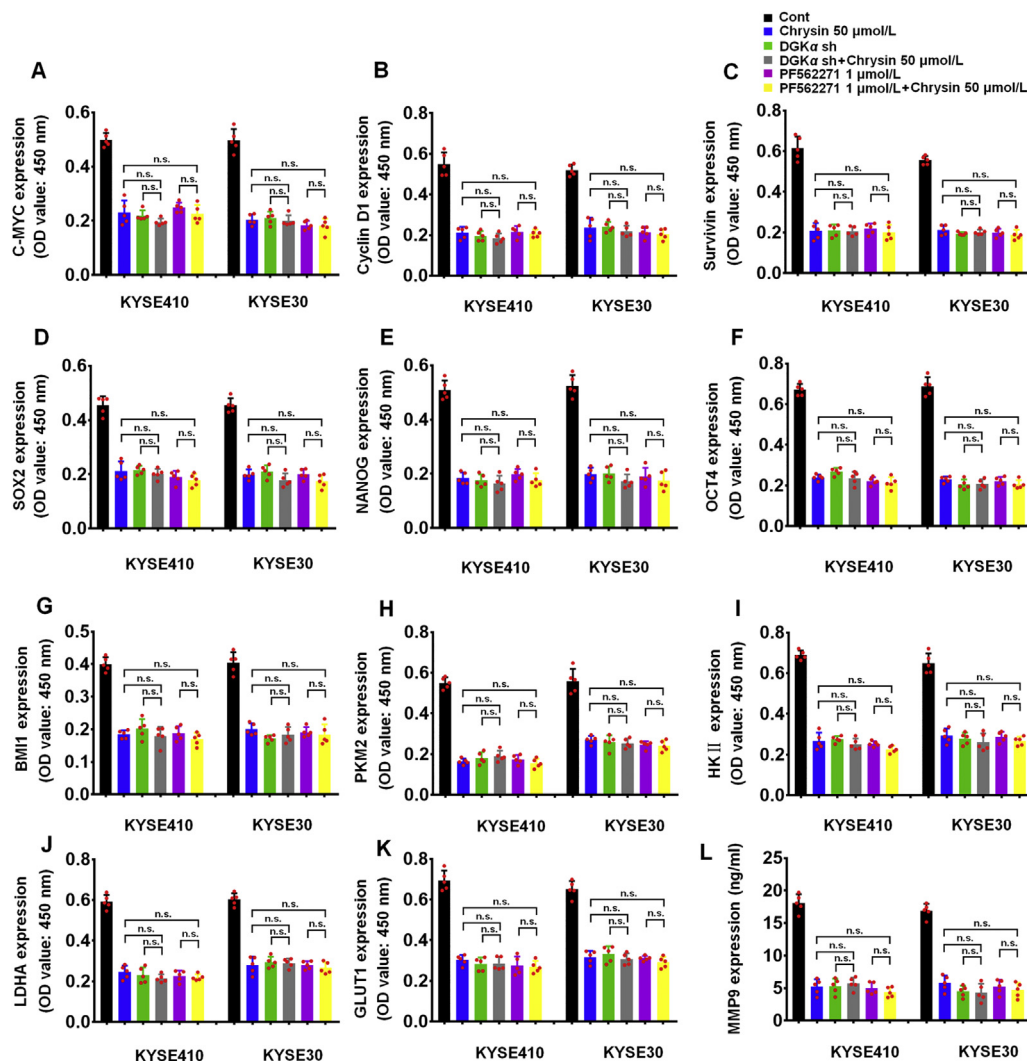


**Figure 6** Chrysin inhibits the expression of downstream malignant effectors *via* DGK $\alpha$ /FAK complex. (A)–(L) The indicated control or DGK $\alpha$  shRNA or 1  $\mu$ mol/L PF562271-incubated ESCC cells were treated with 50  $\mu$ mol/L chrysin. The intratumoral expression of C-MYC (A), cyclin D1 (B), survivin (C), SOX2 (D), NANOG (E), OCT4 (F), BMI1 (G), PKM2 (H), HKII (I), LDHA (J), GLUT1 (K), and the secretion of MMP9 in supernatant (L) were evaluated using quantitative ELISA assay. n.s., no significant difference. Error bars, mean  $\pm$  SD of five independent experiments.

Fig. S3 further shows that chrysin dose-dependently suppressed the phosphorylation of JAK2 Tyr1007/1008 and JAK3 Tyr980/981 in ESCC cells.

### 3.4. DGK $\alpha$ Asp 435 site contributes to chrysin-mediated disruption of DGK $\alpha$ /FAK complex in ESCC cells

DGK $\alpha$  interacts with FAK FERM domain *via* its catalytic domain and activates FAK in ESCC cells<sup>5</sup>. We evaluated whether chrysin-inhibited FAK activation is majorly dependent on the disruption of DGK $\alpha$ /FAK complex. The homology model of the catalytic domain of human DGK $\alpha$  and molecular docking analysis were used to evaluate the interaction between chrysin and DGK $\alpha$  (Fig. 4A and B). Molecular docking analysis indicated that chrysin covalently bound to Asp 435 site in the catalytic domain of DGK $\alpha$  (Fig. 4C and D). Immunoprecipitation and confocal assays show that chrysin dose-dependently suppressed the interaction between the DGK $\alpha$  and FAK and the phosphorylation of FAK Tyr397 in

the indicated ESCC cells (Fig. 4E and F). We further examined whether Asp435 site in DGK $\alpha$  is contributed to chrysin-mediated disruption of DGK $\alpha$ /FAK complex. Immunoprecipitation and quantitative ELISA assays show that DGK $\alpha$  D435E mutant plasmid abolished chrysin-disrupted DGK $\alpha$ /FAK complex (Fig. 4G) and the phosphorylation of FAK Tyr397 (Fig. 4H). MTS assay shows that DGK $\alpha$  D435E mutant partially abolished the inhibitory effect of 50  $\mu$ mol/L chrysin on cell growth in the indicated ESCC cells (Supporting Information Fig. S4). Taken together, the Asp435 site in catalytic domain of DGK $\alpha$  is critical for chrysin-mediated disruption of DGK $\alpha$ /FAK complex and inhibition of the FAK Tyr397 site phosphorylation in ESCC cells.

### 3.5. DGK $\alpha$ /FAK complex is the intracellular target mediating the tumor inhibitory effect of chrysin

Then, we examined the inhibitory effect of chrysin on the phosphorylation of FAK/AKT pathway and proliferation of ESCC cells

in the presence of DGK $\alpha$  shRNA. Fig. 5A–D shows that 50  $\mu\text{mol/L}$  chrysin could not further inhibit cell growth and FAK/AKT activation in DGK $\alpha$ -depleted ESCC cells.

To explore the mechanism by which chrysin disrupts DGK $\alpha$ /FAK complex in ESCC cells, we assessed the inhibitory effect of chrysin on downstream effectors in ESCC cells using quantitative ELISA assays. As shown in Fig. 6A–L, DGK $\alpha$  shRNA or 1  $\mu\text{mol/L}$  FAK inhibitor-PF562271 effectively downregulated the expression of proliferation-related proteins, such as C-MYC (Fig. 6A), cyclin D1 (Fig. 6B), or survivin (Fig. 6C), stemness-related proteins, such as SOX2 (Fig. 6D), NANOG (Fig. 6E), OCT4 (Fig. 6F), or BMI1 (Fig. 6G), glycolysis-related molecules, including PKM2 (Fig. 6H), HKII (Fig. 6I), LDHA (Fig. 6J), or GLUT1 (Fig. 6K), and metastasis-related protein MMP9 (Fig. 6L). However, 50  $\mu\text{mol/L}$  chrysin could not further inhibit the expression of these proteins in the presence of DGK $\alpha$  shRNA or PF562271 (Fig. 6A–L).

### 3.6. Chrysin inhibits the malignancy of ESCC tumor in vivo

To extend our *in vitro* observations, we assessed whether chrysin inhibited ESCC progression *in vivo*. The indicated ESCC cells (approximately  $2.5 \times 10^6$  cells for each cell line) were subcutaneously inoculated into the right flank of 5-week-old female nude mice. When tumor grew to 80–100  $\text{mm}^3$ , the animals were treated with different doses of chrysin (10, 25, and 50  $\text{mg/kg/day}$ , *p.o.*). After 26-day treatment, chrysin dose-dependently reduced the growth of ESCC tumors (Fig. 7A) and upregulated the expression of cleaved PARP or caspase 3 (Fig. 7B and C). Chrysin also effectively downregulated the activation of FAK/AKT signaling axis in ESCC tumors evaluated using quantitative ELISA assays (Fig. 7D–G). Histological analysis of heart, liver, spleen and kidney tissues shows no alterations between control group and chrysin treatment groups, suggesting that chrysin did not produce and toxic effects in normal tissues (Fig. 7H). The difference of

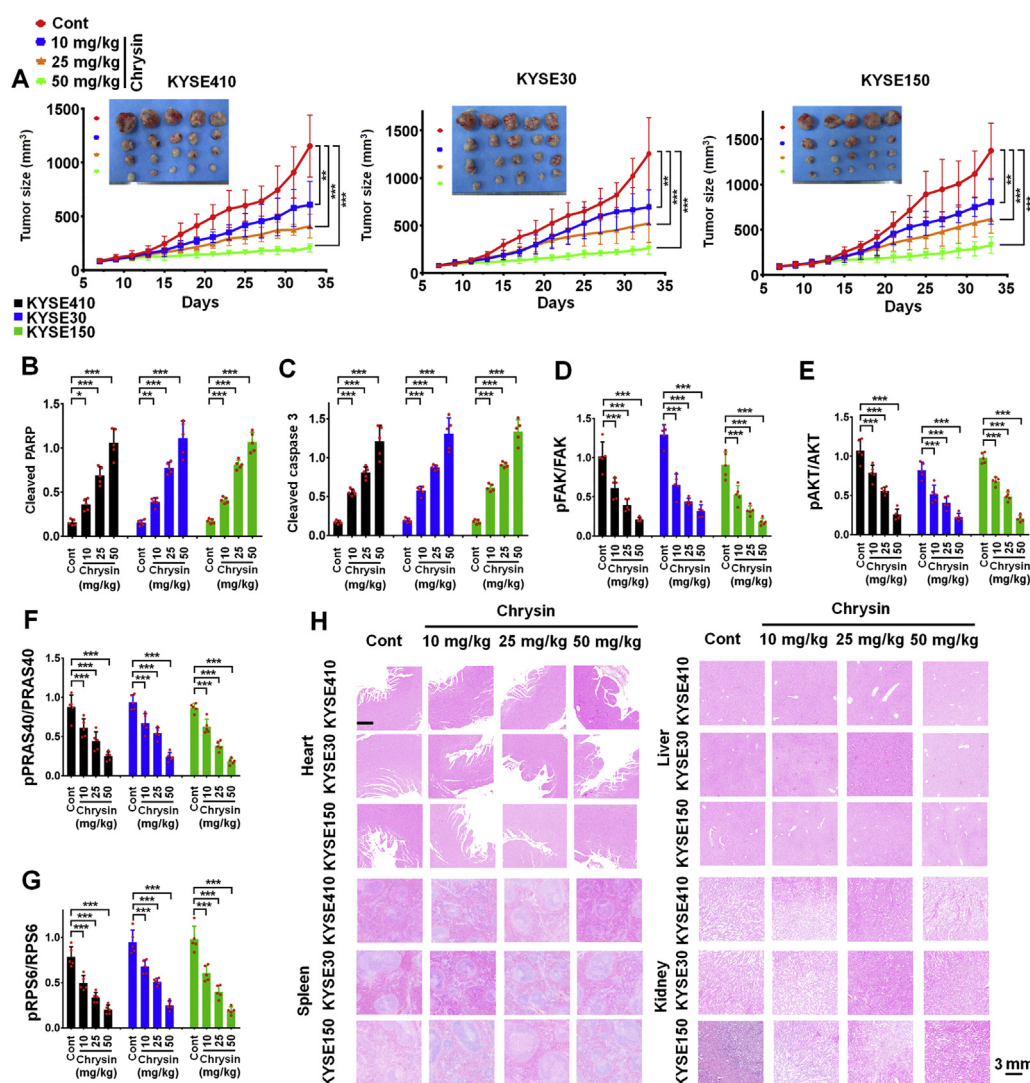


**Figure 7** Chrysin suppresses the proliferation and promotes apoptosis of ESCC tumors *in vivo*. (A) Animals harbored the indicated ESCC tumors were treated different doses of chrysin (10, 25, and 50  $\text{mg/kg/day}$ , *p.o.*). The growth curves and representative images of tumor were shown. (B)–(G) Cleaved PARP (B), cleaved caspase 3 (C), and pFAK Tyr<sup>397</sup>/FAK (D), pAKT Ser<sup>473</sup>/AKT (E), pPRAS40 Thr<sup>246</sup>/PRAS40 (F), or pRPS6 Ser<sup>235/236</sup>/RPS6 (G) ratio in the indicated tumors was evaluated using quantitative ELISA assay. (H) Histopathologic analyses of major organs, including heart, liver, spleen, or kidney from control and different doses of chrysin (10, 25, and 50  $\text{mg/kg/day}$ , *p.o.*). Magnification, 3 mm as indicated. \* $P < 0.05$ ; \*\* $P < 0.01$ ; \*\*\* $P < 0.001$ . Error bars, mean  $\pm$  SD of five independent experiments.

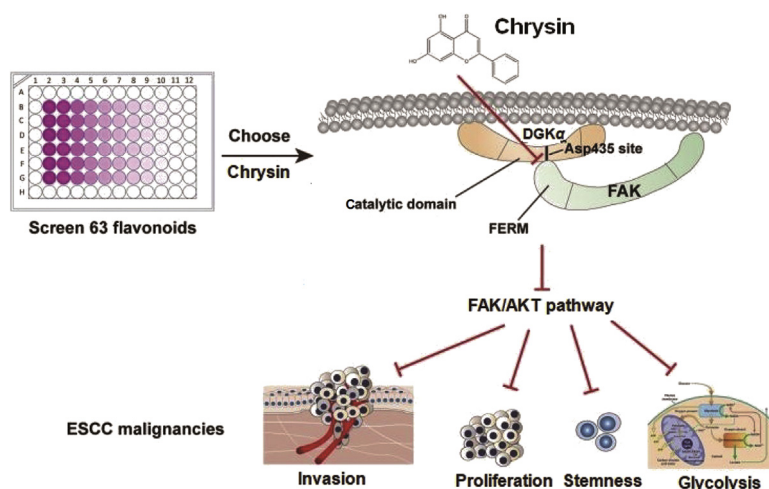


**Figure 8** Proposed model of chrysin-mediated anti-ESCC effect. Chrysin inhibited several malignant phenotypes, including proliferation, invasion, stemness, and glycolysis, in ESCC cells. Mechanistically, chrysin disrupted the formation of DGK $\alpha$ /FAK signalosome *via* interacting with the Asp<sup>435</sup> site in the catalytic domain of DGK $\alpha$  and subsequently inhibited the phosphorylation of FAK Tyr<sup>397</sup> site, suppressed the activation of FAK/AKT pathway and its controlled downstream tumor-promoting effectors in ESCC cells.

body weight between chrysin treatment groups and control group is minimal (Supporting Information Fig. S5).

#### 4. Discussion

Chrysin, a flavonoid compound, has been reported to possess multiple biological effects on suppressing tumorigenesis<sup>11,12,14</sup>. However, the potential mechanism remains poorly understood. In this study, we have demonstrated that chrysin disrupted the assembly of DGK $\alpha$ /FAK complex to inhibit FAK/AKT signaling, and resultantly exerted tumor inhibitory effect on ESCC cells both *in vitro* and *in vivo*, while had no or little toxic effect on normal cells. Importantly, mechanistic analysis suggested that the Asp 435 site in catalytic domain of DGK $\alpha$  was critical for chrysin-mediated disruption of DGK $\alpha$ /FAK complex. Various natural products exert their tumoricidal activities *via* activating apoptosis<sup>22,23</sup>. We found that chrysin initiated apoptotic cell death in ESCC cells, which was supported by the results of FITC/PI double staining and caspase 3/7 activity. The increase in apoptotic rate was also reflected by the cleavage of PARP. Furthermore, blockage of caspase pathway by Z-VAD-FMK markedly abolished the tumor-inhibitory effect of chrysin.

The FAK/AKT pathway is often dysregulated in cancers and critically contributes to tumor malignancy<sup>4,5,24,25</sup>. Therefore, FAK/AKT axis can serve as an attractive target for intervention of tumorigenesis<sup>26</sup>. Several studies have noted that chrysin treatment leads to a downregulation of AKT signaling<sup>27–29</sup>. Here, we showed that chrysin effectively inhibited the activation of FAK/AKT signaling in ESCC cells. However, the molecular details concerning the mechanism by which chrysin disrupted FAK/AKT signaling remained to be further defined in the future. We recently extended this observation by showing that DGK $\alpha$  and FAK were able to form the oncogenic unit in ESCC cells to activate FAK/AKT signaling<sup>5</sup>. In the present study, we have provided evidences that chrysin disrupted the oncogenic DGK $\alpha$ /FAK complex,

resulting in inhibition of FAK/AKT signaling and tumor malignant progression. Furthermore, our results clarified several previously unclear areas of signaling changes caused by chrysin. We found that chrysin was located in the pocket of DGK $\alpha$  catalytic domain (amine acid 375–506) to covalently bind with Asp 435 site in DGK $\alpha$ , and disrupted the interaction between DGK $\alpha$  and FAK to inactivate FAK/AKT signaling. Importantly, we observed that chrysin treatment-induced antisignaling and tumor inhibitory effect could not be enhanced in the DGK $\alpha$ -depleted or FAK inhibitor-treated ESCC cells, suggesting that DGK $\alpha$ /FAK complex may possibly be the intracellular target mediating the tumor inhibitory effect of chrysin. However, due to the lack of biochemical data, we cannot fully conclude the direct binding of chrysin to DGK $\alpha$ . Mutational and structural studies will be used to evaluate the structural mechanism by which chrysin affects DGK $\alpha$ 's function in our future study. Interestingly, our PTKs antibody array results showed that chrysin inhibited some other kinases, in addition to FAK. We suggest that chrysin could be potentially applied to inhibit several protein kinases. Future biochemical, cellular assays and *in vivo* experiments are warranted to search and evaluate other intracellular targets and relevant anti-cancer activities of chrysin. Combining these believes together, we hypothesized that some of the previously undescribed signaling regulatory mechanisms mediated by DGK $\alpha$ , such as controlling the activation of tyrosine kinases, might still be valid in some context.

In the present study, the potential tumor-promoting effect of DGK $\alpha$ /FAK axis is further evaluated by observing the changes of DGK $\alpha$ -controlled downstream effectors, whose functions include inducing glycolysis, increasing stemness activity, as well as promoting tumor proliferation and metastasis. In various previous studies, the disorder of these molecules has been associated with tumor progression and poor patient prognosis both in preclinical and clinical levels<sup>30–33</sup>. Importantly, chrysin can suppress the expression of these proteins *via* inhibition of DGK $\alpha$ /FAK activity. Therefore, our findings provide deep insights into the mechanisms

underlying chrysin-mediated inhibition of ESCC malignancy, further supporting that DGK $\alpha$ /FAK complex can act as an intracellular target mediating the antitumor effect of chrysin.

In summary, the present study has illustrated DGK $\alpha$ /FAK complex as a target of chrysin. Chrysin may possibly bind to the Asp<sup>435</sup> in the catalytic domain of DGK $\alpha$  to inhibit its interaction with FAK, thus suppressing the activation of FAK/AKT signaling axis and ESCC progression both *in vitro* and *in vivo*. This study provides new insights for a throughout understanding of the molecular mechanisms of chrysin in anticancer effects and offers a new direction for the development of natural products-derived small-molecule inhibitors of FAK-related protein complex (Fig. 8).

## 5. Conclusions

Chrysin exerts its anticancer effect in ESCC cells *via* disruption of the assembly of DGK $\alpha$ /FAK complex and resultant blockage of the FAK/AKT signaling pathways. Therefore, chrysin may be a promising candidate for ESCC treatment.

## Acknowledgments

This work was supported by the National Natural Science Foundation of China (81830086, 81988101, 81772504 and 81972243), Beijing Municipal Commission of Health and Family Planning Project (PXM2018\_026279\_000005, China).

## Author contributions

Qimin Zhan designed the experiments and wrote the paper. Jie Chen, Yan Wang, Weimin Zhang, Di Zhao, Lingyuan zhang, Jiawen Fan, and Jinting Li performed the experiments and analyzed the data.

## Conflicts of interest

The authors declare no conflicts of interest.

## Appendix A. Supporting information

Supporting data to this article can be found online at <https://doi.org/10.1016/j.apsb.2020.07.011>.

## References

- Chen W, Zheng R, Baade PD, Zhang S, Zeng H, Bray F, et al. Cancer statistics in China. *Ca Cancer J Clin* 2016;**66**:115–32.
- Zeng H, Chen W, Zheng R, Zhang S, Ji JS, Zou X, et al. Changing cancer survival in China during 2003–15: a pooled analysis of 17 population-based cancer registries. *Lancet Glob Health* 2018;**6**:e555–67.
- Zhou B, Wang GZ, Wen ZS, Zhou YC, Huang YC, Chen Y, et al. Somatic mutations and splicing variants of focal adhesion kinase in non-small cell lung cancer. *J Natl Cancer Inst* 2018;**110**:195–204.
- Liu SC, Hus T, Chang YS, Chuang AK, Jiang SS, OuYang CN, et al. Cytoplasmic LIF reprograms invasion mode to enhance NPC dissemination through modulating YAP1-FAK/PXN signaling. *Nat Commun* 2018;**9**:5105.
- Chen J, Zhang W, Wang Y, Zhao D, Wu M, Fan J, et al. The diacylglycerol kinase  $\alpha$  (DGK $\alpha$ )/AKT/NF- $\kappa$ B feedforward loop promotes esophageal squamous cell carcinoma (ESCC) progression *via* FAK-dependent and FAK-independent manner. *Oncogene* 2019;**38**:2533–50.
- Golubovskaya VM, Finch R, Zheng M, Kurenova EV, Cance WG. The 7-amino-acid site in the proline-rich region of the N-terminal domain of p53 is involved in the interaction with FAK and is critical for p53 functioning. *Biochem J* 2008;**411**:151–60.
- Golubovskaya VM, Palma NL, Zheng M, Ho B, Magis A, Ostrov D, et al. A small-molecule inhibitor, 5'-O-tritylthymidine, targets FAK and Mdm-2 interaction, and blocks breast and colon tumorigenesis *in vivo*. *Anticancer Agents Med Chem* 2013;**13**:532–45.
- Mann J. Natural products in cancer chemotherapy: past, present and future. *Nat Rev Canc* 2002;**2**:143–8.
- Fu B, Wang N, Tan HY, Li S, Cheung F, Feng Y. Multi-component herbal products in the prevention and treatment of chemotherapy-associated toxicity and side effects: a review on experimental and clinical evidences. *Front Pharmacol* 2018;**9**:1394.
- Guerra AR, Duarte MF, Duarte IF. Targeting tumor metabolism with plant-derived natural products; emerging trends in cancer therapy. *J Agric Food Chem* 2018;**66**:10663–85.
- Khoo BY, Chua SL, Balaran P. Apoptotic effects of chrysin in human cancer cell lines. *Int J Mol Sci* 2010;**11**:2188–99.
- Yang B, Huang J, Xiang T, Yin X, Luo X, Huang J, et al. Chrysin inhibits metastatic potential of human triple-negative breast cancer cells by modulating matrix metalloproteinase-10, epithelial to mesenchymal transition, and PI3K/AKT signaling pathway. *J Appl Toxicol* 2014;**34**:105–12.
- Kasala ER, Bodduluru LN, Madana RM, AK V, Gogoi R, Barua CC. Chemopreventive and therapeutic potential of chrysin in cancer: mechanistic perspectives. *Toxicol Lett* 2015;**233**:214–25.
- Xu D, Jin J, Yu H, Zhao Z, Ma D, Zhang C, et al. Chrysin inhibited tumor glycolysis and induced apoptosis in hepatocellular carcinoma by targeting hexokinase-2. *J Exp Clin Oncol* 2017;**36**:44.
- Sun LP, Chen AL, Hung HC, Chien YH, Huang JS, Huang CY, et al. Chrysin: a histone deacetylase 8 inhibitor with anticancer activity and a suitable candidate for the standardization of Chinese propolis. *J Agric Food Chem* 2012;**60**:11748–58.
- Lin CC, Yu CS, Yang JS, Lu CC, Chiang JH, Lin JP, et al. Chrysin, a natural and biologically active flavonoid, influences a murine leukemia model *in vivo* through enhancing populations of T- and B-cells, and promoting macrophage phagocytosis and NK cell cytotoxicity. *In Vivo* 2012;**26**:665–70.
- Cao J, Lv W, Wang L, Xu J, Yuan P, Huang S, et al. Ricolinostat (ACY-1215) suppresses proliferation and promotes apoptosis in esophageal squamous cell carcinoma *via* miR-30d/PI3K/AKT/mTOR and ERK pathways. *Cell Death Dis* 2018;**9**:817.
- Lu XY, Chen DL, Wang DS, Chen LZ, Mo HY, Sheng H, et al. Melatonin enhances sensitivity to fluorouracil in oesophageal squamous cell carcinoma through inhibition of Erk and AKT pathway. *Cell Death Dis* 2016;**7**:e2432.
- Chen X, Ying Z, Lin X, Lin H, Wu J, Li M, et al. Acylglycerol kinase augments JAK2/STAT3 signaling in esophageal squamous cells. *J Clin Invest* 2013;**123**:2576–89.
- Hu N, Kadota M, Liu H, Abnet CC, Su H, Wu H, et al. Genomic landscape of somatic alterations in esophageal squamous cell carcinoma and gastric cancer. *Canc Res* 2016;**76**:1714–23.
- Johnson DE, O'Keefe RA, Grandis JR. Targeting the IL-6/JAK/STAT3 signalling axis in cancer. *Nat Rev Clin Oncol* 2018;**15**:234–48.
- Guzmán EA. Regulated cell death signaling pathways and marine natural products that target them. *Mar Drugs* 2019;**17**:E76. pii.
- Wang Y, Zhong J, Bai J, Tong R, An F, Jiao P, et al. The application of natural products in cancer therapy by targeting apoptosis pathways. *Curr Drug Metabol* 2018;**19**:739–49.
- Song M, Bode AM, Dong Z, Lee MH. AKT as a therapeutic target for cancer. *Canc Res* 2019;**79**:1019–31.
- Sulzmaier FJ, Hean C, Schlaepfer DD. FAK in cancer: mechanistic findings and clinical applications. *Nat Rev Canc* 2014;**14**:598–610.
- Lee BY, Timpson P, Horvath LG, Daly RJ. FAK signaling in human cancer as a target for therapeutics. *Pharmacol Ther* 2015;**146**:132–49.

27. Ryu S, Lim W, Bazer FW, Song G. Chrysin induces death of prostate cancer cells by inducing ROS and ER stress. *J Cell Physiol* 2017;**232**: 3786–97.
28. Park W, Park S, Lim W, Song G. Chrysin disrupts intracellular homeostasis through mitochondria-mediated cell death in human choriocarcinoma cells. *Biochem Biophys Res Commun* 2018;**503**: 3155–61.
29. Fu B, Xue J, Li Z, Shi X, Jiang BH, Fang J. Chrysin inhibits expression of hypoxia-inducible factor-1 $\alpha$  through reducing hypoxia-inducible factor-1 $\alpha$  stability and inhibiting its protein synthesis. *Mol Canc Therapeut* 2007;**6**:220–6.
30. VanArsdale T, Boshoff C, Arndt KT, Abraham RT. Molecular pathways: targeting the cyclin D-CDK4/6 axis for cancer treatment. *Clin Canc Res* 2015;**21**:2905–10.
31. Wang J, Ye C, Chen C, Xiong H, Xie B, Zhou J, et al. Glucose transporter GLUT1 expression and clinical outcome in solid tumors: a systematic review and meta-analysis. *Oncotarget* 2017;**8**:16875–86.
32. Hüser L, Novak D, Umansky V, Altevogt P, Utikal J. Targeting SOX2 in anticancer therapy. *Expert Opin Ther Targets* 2018;**22**:983–91.
33. Winer A, Adams S, Mignatti P. Matrix metalloproteinase inhibitors in cancer therapy: turning past failures into future successes. *Mol Canc Therapeut* 2018;**17**:1147–55.